RESEARCH PAPER

Acta Neurobiol Exp 2022, 82: 96–105
DOI: 10.55782/ane-2022-009

Identification of microRNA/target gene in the dentate gyrus of 7-day-old mice following isoflurane exposure

Bing-Nan Yang[1,2#], Chu-Tong Zhang[3#], Le-Fan Liu[4#], Xiao-Lin Wu[5], Hai-Bo Hu[5], Yu Chen[1,2], Muneeb Iqbal[6], Yan-Bing Ma[5], Jin-Song Zhou[5], Xin-Li Xiao[5,*], Jian-Xin Liu[1,2*]

[1] Institute of Neurobiology, School of Basic Medical Sciences, Xi'an Jiaotong University Health Science Center, Xi'an, China,
[2] Institute of Neuroscience, Translational Medicine Institute, Xi'an Jiaotong University Health Science Center, Xi'an, China,
[3] Qide College, Xi'an Jiaotong University Health Science Center, Xi'an, China,
[4] School of Laboratory Medicine, Hubei University of Chinese Medicine, Wuhan, China,
[5] Department of Human Anatomy, Histology and Embryology, School of Basic Medical Sciences, Xi'an Jiaotong University Health Science Center, Xi'an, China,
[6] R & D Biology, KIPS Head Office, Lahore, Pakistan,
[#] These authors contribute to this work equally,
** Email: liujianxin@mail.xjtu.edu.cn*

Studies on rodents and nonhuman primates suggest that exposure to anesthetics, particularly in the young brain, is associated with neuronal apoptosis as well as hippocampal-dependent cognitive dysfunction. Disruption of the development of dentate gyrus may play an important role in anesthetics-induced neurotoxicity. However, the anesthetics triggered molecular events in the dentate gyrus of the developing brain are poorly understood. By integrating two independent data sets obtained from miRNA-seq and mRNA-seq respectively, this study aims to profile the network of miRNA and potential target genes, as well as relevant events occurring in the dentate gyrus of isoflurane exposed 7-day-old mice. We found that a single four hours exposure to isoflurane yielded 1059 pairs of differently expressed miRNAs/target genes in the dentate gyrus. Gene ontology and Kyoto Encyclopedia of Genes and Genomes enrichment analysis further indicates that dysregulated miRNAs/target genes have far-reaching effects on the cellular pathophysiological events, such as cell apoptosis, axon development, and synaptic transmission. Our results would greatly broaden our functional understanding of the role of miRNA/target gene in the context of anesthetics-induced neurotoxicity.

Key words: anesthetics, isoflurane, dentate gyrus, miRNA expression profiles

INTRODUCTION

Animal studies have shown that volatile anesthetics such as isoflurane, sevoflurane, and desflurane can cause neuronal apoptosis as well as mostly hippocampal-dependent cognitive dysfunction in the developing brain (Loepke et al., 2009; Fang et al., 2012; Li et al., 2015; Armstrong et al., 2017). Moreover, the possibility of anesthetics-induced neurotoxicity in children has led to concerns about the safety of pediatric anesthesia (Armstrong et al., 2017; McCann et al., 2019). The dentate gyrus, where the neuronal proliferation continues postnatally, is responsible for the exceptional structural plasticity of the hippocampus (Cameron and Glover, 2015). Initiation of intrinsic pathways of the apoptotic cell death in the dentate gyrus was found to be partly responsible for the neurocognitive neurotoxicity after the anesthetics exposure (Lee et al., 2014; Xiao et al., 2021). However, the underlying anesthetics-triggered molecular events in the dentate gyrus are poorly understood.

miRNAs are small, non-coding, single-stranded nucleic acids that play an important gene-regulatory role

Received 11 October 2021, accepted 29 December 2021

by binding to the mRNAs to induce their repression (Bartel, 2004; 2018). miRNAs are loaded onto RNA-induced silencing complex (RISC) by binding to the 3'-UTR of the protein-coding mRNA transcripts, leading to reduced translational efficiency (Bartel, 2018; Bartel, 2004). A single miRNA can target multiple mRNAs, thus having far-reaching effects on cellular pathophysiological events (Bartel, 2004). Although miRNAs have been reported to involve in anesthetics-induced neurotoxicity and neurocognitive deficit (Sun et al., 2020; Bahmad et al., 2020), their specific functions in this context are only beginning to be elucidated. A detailed profile of dysregulated miRNAs and their target genes in the dentate gyrus will definitely guide our understanding of this issue.

By integrating two independent data sets obtained from miRNA-seq and mRNA-seq, this study will explicitly profile the miRNAs as well as their target genes in the dentate gyrus of 7-day-old mice following exposure to isoflurane, one of the most popular anesthetics used in the field of pediatrics. Gene ontology (GO) and Kyoto Encyclopedia of Genes and Genomes (KEGG) analysis was performed to identify miRNA/target genes that potentially mediate isoflurane-induced neurotoxicity, with particular regard to cell apoptosis.

METHODS

Animals

Swiss male mice on postnatal day 7 (P7) were used in this study. The animal protocol was approved by the Experimental Animal Center of Xi'an Jiaotong University Health Science Center (certificate no. 22-9601018), and all mice were treated in strict accordance with APS/NIH guidelines. The experimental design was accepted by the Animal Care and Use Regulation of Xi'an Jiaotong University Health Science Center. The mice were housed with free access to food and water on a 12-h light/dark cycle.

Isoflurane exposure

Eight of P7 mice were randomly divided into isoflurane and control groups. The isoflurane-exposed group received 1.5% isoflurane (Lunan Bert Pharmaceutical Group Corporation, Shanghai, China) in 1 L per minute of gas mixture (50% O_2 and 50% air) in a plastic chamber for 4 h. The size of the anesthesia chamber, used in this study, was 20 × 20 × 10 cm. The chamber was kept in a homoeothermic incubator to maintain the experimental temperature at 37°C. We observed responses of mice to tail clamping every 15 min under anesthesia. The concentrations of oxygen, carbon dioxide, and isoflurane in the chamber were continuously monitored by using an infrared gas analyzer (Drägerwerk AG, Germany). Meanwhile, respiratory rate, skin color, and body movements were also observed. The control mice were placed in the anesthesia chamber for 4 h without exposing them to the anesthetic agent but all other conditions were identical to those provided to the isoflurane group. After this, the mice were placed along with their mother.

Tissue collection and RNA preparation

12 h after exposure, the micro-dissected dentate tissues were prepared for RNA-seq or real-time PCR analysis. Following deep anesthesia with chloral hydrate (0.4 g/kg), the brains were taken out and cut into 500 μm thick coronal sections with a brain matrix (RWD Life Science Co., Ltd, China) and bilaterally DG tissues were rapidly micro-dissected on ice under a stereomicroscope. Briefly, a transection along the hippocampal fissure on the section was done to separate the dentate gyrus from the rest of the hippocampus. Then, a cut was placed between the dentate gyrus and the ventricular surface on one side and the CA3 region on the other side to free the dentate gyrus tissue. The total RNA was extracted using the total RNA purification kit (LC Sciences, Houston, USA) according to the manufacturer's protocol. The total RNA quantity and purity were analyzed by Bioanalyzer 2100 and RNA 6000 Nano LabChip Kit (Agilent, CA, USA).

miRNA library construction and sequencing

1 μg of total RNA from the micro-dissected dentate gyrus was used to prepare the miRNA library according to the protocol of TruSeq Small RNA Sample Prep Kits (Illumina, San Diego, USA). Then we performed the single-end sequencing (1 x 50 bp) on an Illumina Hiseq2500 at the LC-BIO (Hangzhou, China) following the vendor's protocol. Raw reads were subjected to an in-house program, ACGT101-miR (LC Sciences, Houston, Texas, USA) to remove adapter dimmers, junk, low complexity, common RNA families and repeats. In the next step, unique sequences with 18-26 nucleotides in length were mapped to mouse precursors in miRBase 22.0 by BLAST to identify known miRNAs and novel 3p- and 5p-derived miRNAs. Length variation at both 3' and 5' ends and one mismatch inside the sequence were allowed in the alignment. The unique sequences mapping to mouse mature miRNAs in hairpin arms were identified as known miRNAs, and the unique sequences mapping to the other arm of known mouse precursor hairpin op-

posite to the annotated mature miRNA-containing arm were considered to be novel 5p- or 3p derived miRNA candidates. The remaining sequences were mapped to other selected species precursors in miRBase 22.0 by BLAST search, and the mapped pre-miRNAs were further BLASTed against the mouse genomes to determine their genomic locations. The unmapped sequences were BLASTed against the specific genomes, and the hairpin RNA structures containing sequences were predicated from the flank 80 nt sequences using RNAfold software. Differential expression of miRNAs based on normalized deep-sequencing counts was analyzed by selectively using Fisher exact test, Chi-squared 2 × 2 test, Chi-squared n x n test, Student t-test, or ANOVA based on the design of experiments. The significance threshold was set to be 0.01 and 0.05 in each test.

The prediction of target genes of differently expressed miRNAs

To predict the genes targeted by differently expressed miRNAs, two computational target prediction algorithms (TargetScan 50 and Miranda 3.3a) were used to identify miRNA binding sites. To ensure the accuracy of miRNAs target prediction, the genes ($p<0.05$) predicted by both algorithms were selected.

mRNA library construction and sequencing

Poly(A) RNA was purified from 1μg total RNA using Dynabeads Oligo (dT) 25-61005 (Thermo Fisher, CA, USA). Then the poly(A) RNA was fragmented into small pieces using magnesium RNA fragmentation module (NEB, USA). Then the cleaved RNA fragments were reverse-transcribed to create the cDNA by SuperScript™ II Reverse Transcriptase (Invitrogen, USA), which was followed by synthesizing U-labeled second-stranded DNAs with E. coli DNA polymerase I (NEB, USA), RNase H (NEB, USA) and dUTP Solution (Thermo Fisher, USA). A-base was then added to the blunt ends of each strand, and was ligated to the indexed adapters. Each adapter had a T-base overhang for ligating the adapter to the A-tailed fragmented DNA. Single- or dual-index adapters were ligated to the fragments, and size selection was performed with AMPureXP beads. The U-labeled double-stranded DNAs were treated by heat-labile UDG enzyme (NEB, USA), then the ligated products were amplified with PCR. The average insert size for the final cDNA library was 300±50 bp. Finally, we performed the 2 × 150 bp paired-end sequencing (PE150) on an Illumina Novaseq™ 6000 (LC-Bio Technology CO., Ltd., Hangzhou, China) following the vendor's recommended protocol. Cutadapt software was used to remove the reads that contained adaptor contamination. After removal of the low-quality and undetermined ones, we used HISAT2 software to map reads with mouse genome. The mapped reads of each sample were assembled using StringTie with default parameters. Then, all transcriptomes from all samples were merged to reconstruct a comprehensive transcriptome using GffCompare software. After the final transcriptome was generated, StringTie and Ballgown were used to estimate the expression levels of all transcripts and genes by calculating FPKM. The differentially expressed transcripts and genes were selected with fold change > 2 or fold change < 0.5 and p-value < 0.05 by R package edger or DESeq2.

Identify potential miRNAs/ target genes and GO/ KEGG enrichment analysis

To identify the target mRNA of altered miRNA following isoflurane exposure, the predicted target genes of up-regulated miRNAs were intersected with down-regulated mRNA while the predicted target genes of down-regulated miRNAs were intersected with up-regulated mRNA following isoflurane exposure (Fig. 2A). The mRNAs inside the intersections were selected as target genes. The selected genes were then analyzed by GO and KEGG pathway enrichment. GO enrichment analysis of the selected genes was performed by functional annotation bioinformatics database DAVID 6.8. GO terms (including BP, MF, and CC categories) and KEGG pathways were identified based on a hypergeometric distribution algorithm. The false discovery rate (FDR) was employed for multiple testing corrections using the Benjamini and Hochberg method. The threshold was set as $P<0.05$.

Quantitative real-time PCR (q-PCR) analysis

q-PCR was conducted to validate the accuracy of RNA-seq data. Three of up-regulated miRNAs, 3 of down-regulated miRNAs, 2 of up-regulated mRNAs and 2 of down-regulated miRNAs were randomly selected for q-PCR validation. U6 snRNA was used as an internal control for quantification of the relative expression of miRNAs. 1 μg of total RNA was reverse transcribed into cDNA using the PrimeScript RT reagent Kit (Takara, Japan). q-PCR and data collection were performed in the iQ™5 system (Bio-Rad, USA) using TB Green Premix Ex Taq™ GC kit (Takara, Japan). Cycle threshold values were obtained from the Bio-Rad iQ5 2.0 standard edition optical system software (Bio-Rad, USA). The relative expression of each gene was calculated using the 2DDCT method.

RESULTS

Differently expressed miRNAs in the dentate gyrus following isoflurane exposure

We identified 61 differently expressed miRNAs in the dentate gyrus between isoflurane and control groups through miRNA-seq analysis, including 37 down-regulated miRNA and 24 up-regulated miRNAs in the isoflurane group when compared with the control group (Fig. 1A, B) (Supplementary file 1: Differentially Expressed miRNAs).

Prediction of target genes of differently expressed miRNAs

A total of 10707 genes were selected by the two target prediction algorithms (TargetScan 50 and Miranda 3.3a) to be the potential target genes of down-regulated miRNA following isoflurane exposure (Supplementary File 3: Predicted Target genes of Down-regulated miRNAs), while 12780 genes were selected as the potential target genes of up-regulated miRNAs (Supplementary File 4: Predicted Target genes of Up-regulated miRNAs) (Fig. 2A). Because a single gene might be predicted as the target of several miRNAs, the repeated genes have not been re-numbered repeatedly. Therefore, the number of target genes mentioned above was fewer than those in the excel lists of Supplementary File 3 and 4.

Differently expressed mRNAs in the dentate gyrus following isoflurane exposure

mRNA-seq found 1084 differently expressed mRNAs in the dentate gyrus between the isoflurane and control groups, including 543 down-regulated and 541 up-regulated mRNAs in the isoflurane group when compared with the control group (Fig. 1C, D) (Supplementary File 2: Differentially Expressed mRNAs).

Identification of potential target genes of differentially expressed miRNA in the dentate gyrus following isoflurane exposure

By intersecting the list of predicted target genes of down-regulated miRNAs (or up-regulated) with that of up-regulated mRNAs (or down-regulated) through mRNA-seq, 199 of up-regulated mRNAs were identified as potential target genes of down-regulated miRNAs (Supplementary File 5: Identified Target Genes of Down-regulated miRNAs), and 159 of down-regulated mRNAs were identified as potential target genes of up-regulated miRNAs (Supplementary File 6: Identified Target Genes of Up-regulated miRNAs) in the dentate gyrus following the isoflurane exposure (Fig. 2A). As a single gene might be predicted as the target of several miRNAs, the repeated genes have not been re-numbered.

GO and pathway enrichment of identified target genes

To gain insight into the role of miRNA/target gene in the neurotoxicity of dentate gyrus following isoflurane exposure, the identified target genes of differently expressed miRNAs were further imported into DAVID tool for GO enrichment analysis. GO terms of target genes, have been separately listed regarding the down-regulation (Fig. 2C) or up-regulation of miRNAs (Fig. 2B) following isoflurane exposure (Supplementary File 7: GO Enrichment of Down-regulated miRNAs's Target Genes; Supplementary File 8: GO Enrichment of Up-regulated miRNAs's Target Genes). The detailed KEGG analysis data of the target genes were also separately shown in supplementary (Supplementary File 9: KEGG Enrichment of Down-regulated miRNAs's Target Genes; Supplementary File 10: KEGG Enrichment of Up-regulated miRNAs's Target Genes) regarding the down-regulation (Fig. 2E) or up-regulation of miRNAs (Fig. 2D).

In the dentate gyrus of P7 mice, isoflurane-induced miRNAs/target genes were enriched to a spectrum of cell functions and signal pathways involved in the anesthetic induced neurotoxicity such as apoptosis (Supplementary File 11: miRNAs's Target Genes Related to Apoptotic Process), axon development or guidance (Supplementary File 12: miRNAs's Target Genes Related to Axon Development), inflammatory process (Supplementary File 13: miRNAs's Target Genes Related to inflammatory Response), synaptic transmission or synaptic plasticity (Supplementary File 14: miRNAs's Target Genes Related to Synaptic Transmission or Synaptic Plasticity), and mitochondrial function (Supplementary File 15: miRNAs's Target Genes Related to Mitochondrial Function).

q-PCR validation

Following isoflurane exposure to P7 mice, the up-regulations of mmu-miR-152-3p, mmu-miR-300-3p and mmu-miR-381-3p, and the down-regulations of mmu-miR-129-1-3p, mmu-miR-423-5p and mmu-miR-667-3p in the dentate gyrus were validated by qPCR (Fig. 3A). The mRNA levels of Adam9, Gm6430, Prickle1 and Gm5540 were also consistent with those obtained from mRNA-seq (Fig. 3B).

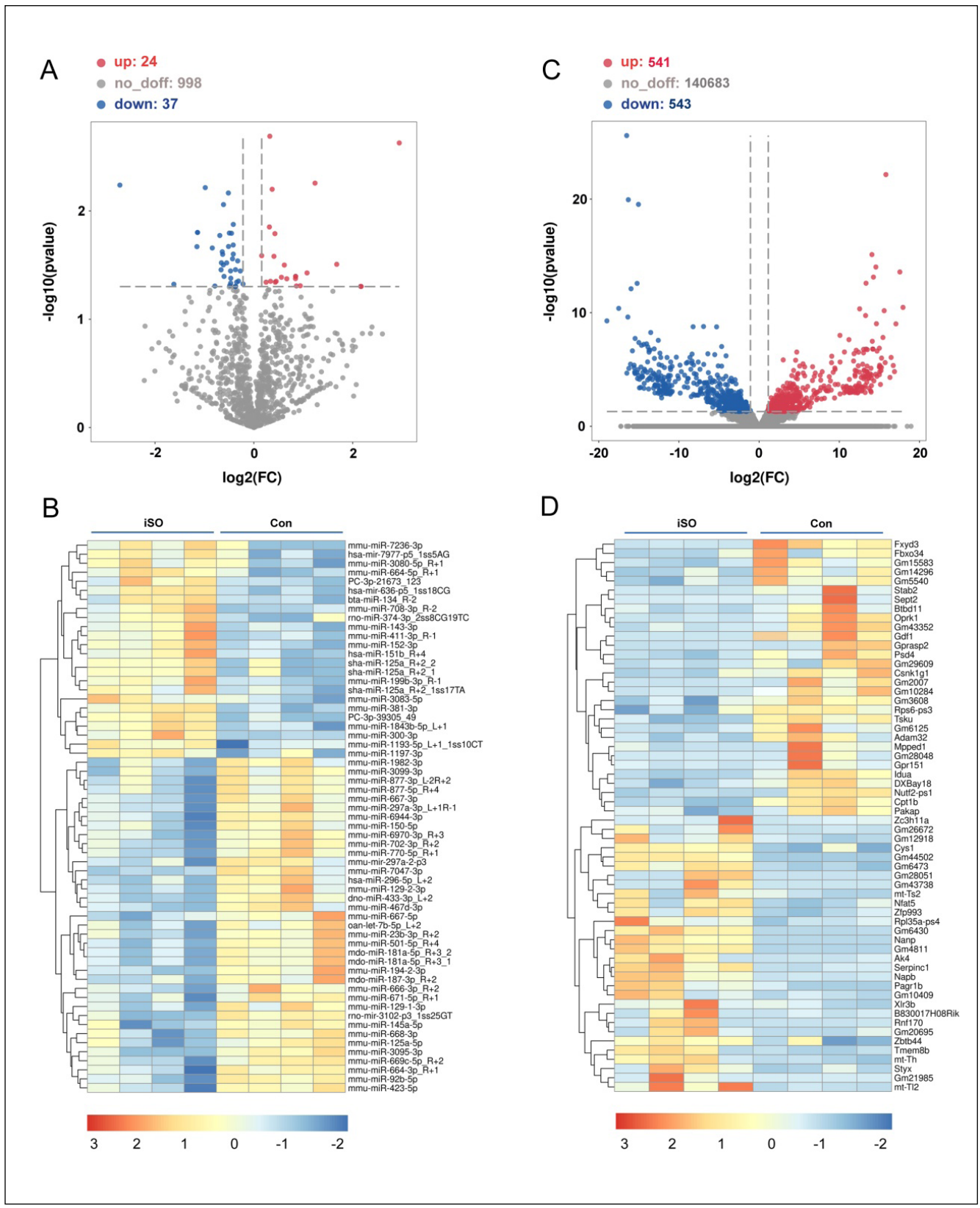

Fig. 1. Volcano plot and Heatmap of differently expressed miRNAs and mRNAs in the dentate gyrus following isoflurane exposure to P7 mice. (A) and (B) Volcano plot and Heatmap of differently expressed miRNA respectively. (C) Volcano plot of differently expressed mRNAs. (D) Heatmap of top 30 up-regulated and down-regulated mRNAs regarding fold changes.

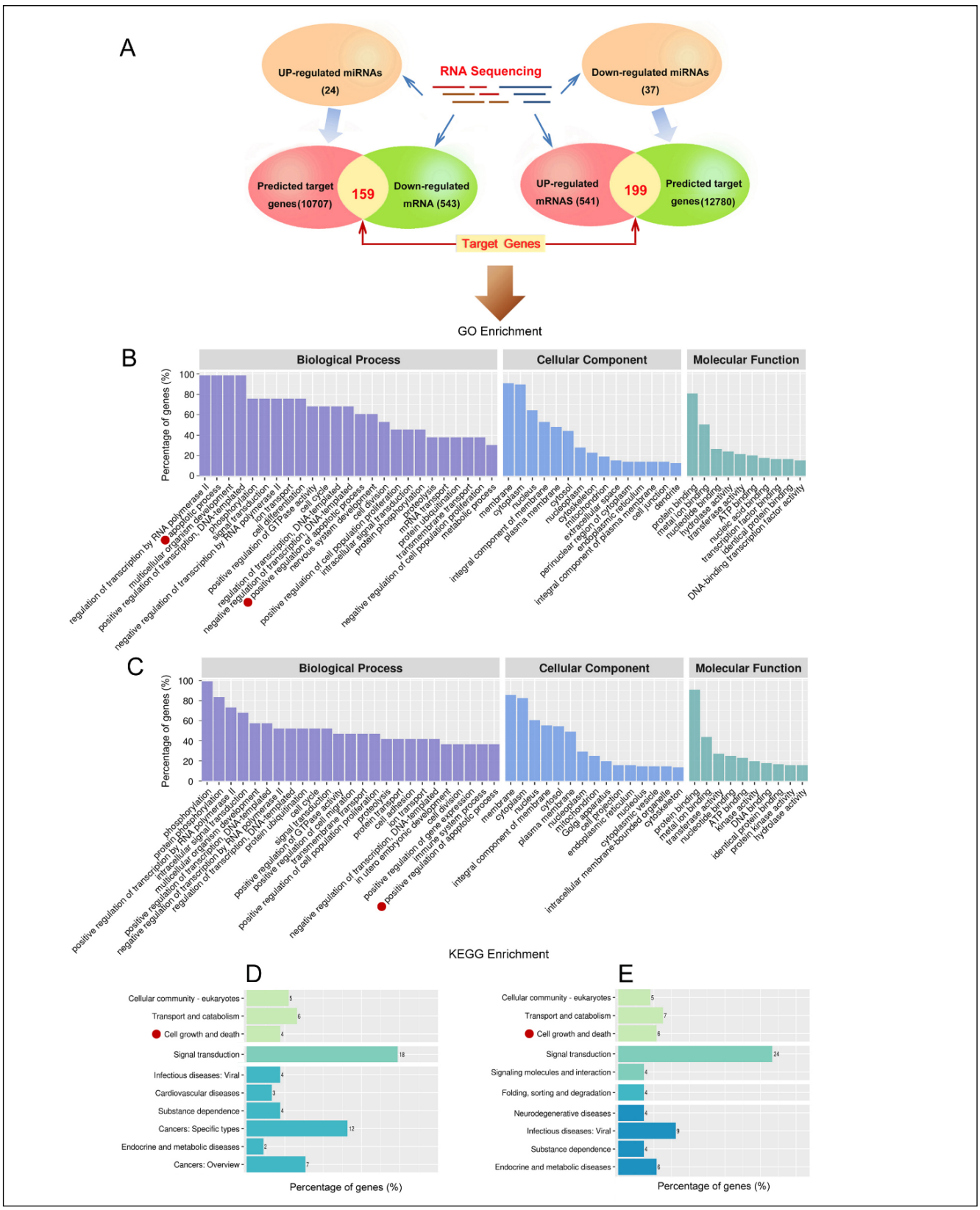

Fig. 2. GO and KEGG enrichment of dysregulated miRNAs-target genes in the dentate gyrus following isoflurane exposure to P7 mice. (A) The outline of logic and results in this study. (B) and (D) GO and KEGG analysis of the target genes of up-regulated miRNAs respectively. (C) and (E) GO and KEGG analysis of the target genes of down-regulated miRNAs respectively.

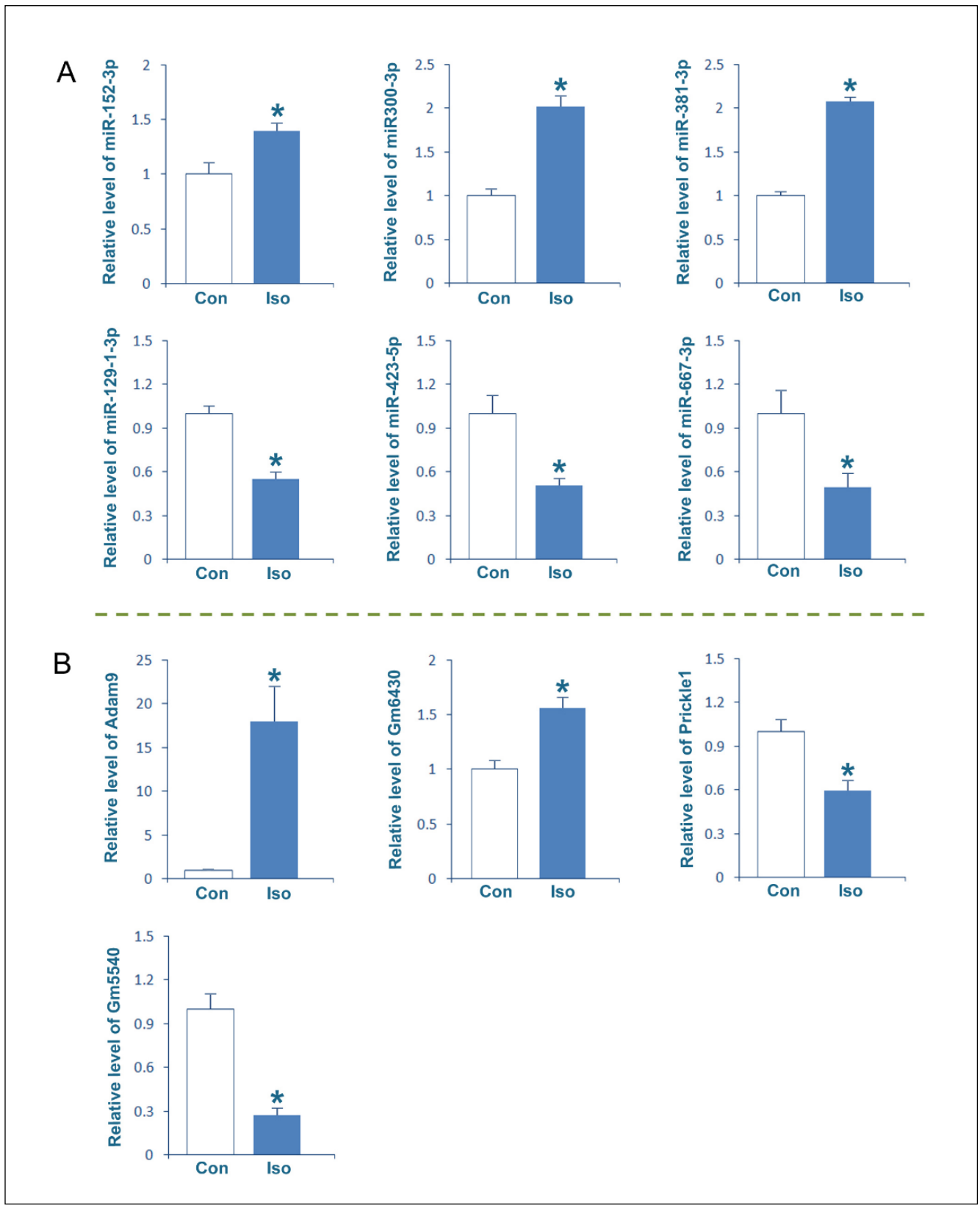

Fig. 3. q-PCR validation. The dysregulations of mmu-miR-152-3p, mmu-miR-300-3p, mmu-miR-381-3p, mmu-miR-129-1-3p, mmu-miR-423-5p and mmu-miR-667-3p are demonstrated (A). The up-regulated mRNAs of Adam9 and Gm6430, and the down-regulated mRNAs of Prickle1 and Gm5540 are also validated (B).

DISCUSSION

Methodological considerations

Several cohort studies with P7 neonatal rodents have demonstrated that administration of anesthetic drugs was associated with consequent neurocognitive deficits (Stratmann et al., 2009; Istaphanous et al., 2011; Tao et al., 2016; Xia et al., 2017). For the rodents, P7 is the peak developmental stage of the tertiary dentate matrix (prominent between days P3 and P10), from where a great increase in the granule cell population during the infantile and juvenile periods is principally derived (Altman and Bayer, 1990). Given that the young and adult rodent do not develop neurocognitive deficits after anesthetics exposure, it is probable that the rodents at the tertiary matrix stage may be more susceptible to anesthetics because the cell proliferation might be disrupted by the exposure (Xiao et al., 2021). In addition, laboratory findings in 7-day-old rodents might provide evidence for human susceptibility to anesthetics-induced neurotoxicity from the third trimester of pregnancy up to the second year of life (Olney et al., 2004; Jevtovic-Todorovic, 2005). Therefore, P7 mice were used in this study to explore miRNAs/target genes mediated molecular events following the isoflurane exposure.

Stratmann et al. (2009) found that the neurocognitive deficit was not observed after 2 h of isoflurane exposure, although noticeable cell death was observed in mice brains, and intervention that caused both cell death and neurocognitive dysfunction was 4 h of isoflurane exposure. Hence, the animals underwent 4 h of isoflurane exposure in this study.

In addition, to ensure the accuracy of miRNAs target prediction, only the genes that were positively predicted by both predicting databases i.e. TargetScan 50 and Miranda 3.3 were included in this study. To identify the potential target genes of miRNAs, the lists of predicted miRNA target genes were further intersected with an independent mRNA database obtained from the dentate gyrus of P7 mice following the isoflurane exposure.

miRNA/target genes are extensively involved in isoflurane-induced neurotoxicity

This is the first study that we are aware of explicit analysis of miRNAs coupling with their target genes in the dentate gyrus following the anesthetics exposure. In the present study, 1059 pairs of differently expressed miRNAs/target genes were identified (Supplementary File 5; Supplementary File 6), suggesting an extensive role of miRNA/target gene in the dentate gyrus of P7 mice following the isoflurane exposure. GO and KEGG enrichment further indicates that isoflurane-induced miRNAs/target genes have far-reaching effects on the cell pathophysiological events such as cell apoptosis (Supplementary File 11), axon development or guidance (Supplementary File 12), inflammatory process (Supplementary File 13), synaptic transmission (Supplementary File 14) and mitochondrial morphogenesis (Supplementary File 15), all of which are potentially involved in developing neurotoxicity. Previous studies have reported the existence of enhanced apoptotic neurodegeneration (Levy, 2017), sustained neuroinflammation (Fodale et al., 2017) as well as disturbed axon development and synaptic transmission (Xu et al., 2019; Atluri et al., 2019) in the brains of anesthetics-exposed animals. Hence, our results strongly support that miRNAs/target genes extensively mediate isoflurane-induced neurotoxicity in the dentate gyrus of P7 mice.

GO and KEGG enrichment found 149 pairs of miRNA/target genes that are involved in an apoptosis-related process or signal pathway (Supplementary File 11), in which a single miRNA always pairs to several genes. The majority of these genes were also targeted by multiple miRNAs. For example, when miR-667-3p pairs to BAK1, Cacna2d2 and Erbb4, the pro-apoptotic protein BAK1 is also potentially targeted by miR-125a-5p, miR-1982-3p, miR-3095-3p, miR-702-3p and miR-7047-3p. This pattern probably indicates an extensive and pivotal role of miRNA in isoflurane-induced cell apoptosis in the dentate gyrus, and makes them promising target for developing strategies for anti-apoptosis induced by anesthetics.

In the rodent hippocampus of the early postnatal period, the granular cells in the dentate gyrus are made up of a heterogeneous population of neurons regarding their original sites, that is, primary dentate neuroepithelium, secondary, and tertiary dentate matrix (Altman and Bayer, 1990). For P7 mice, the new granular cells are massively generated from the tertiary dentate matrix. Our previous study found that 4 h of isoflurane exposure with P7 mice significantly decreased the numbers of nascent cells (1-day-old) originated from the tertiary dentate matrix (Xiao et al., 2021). The findings of apoptosis-related miRNAs/target genes in this study would provide clues for detecting molecular mechanisms underlying the effect mentioned above.

While isoflurane causes a neurotoxic effect in the developing brain under normal condition, it may offer neuroprotection in adult brain suffering with ischemia or infarction through PI3K-Akt, TGF-β/Smad, ERK signal pathways and so on (Neag et al., 2020). Our study of miRNAome investigations in the dentate gyrus may provide clues for understanding the mechanism underlying isoflurane-induced reversed effects on the different brain regions, as well as revealed some novel miRNAs-target

genes involving in the activation/inactivation of these signal pathways following the isoflurane exposure.

Study limitations

First, when we were identifying the target genes, only miRNAs-mRNAs with negative correlation were selected. Actually, both decreased translational efficiency and decreased mRNA level contribute to the miRNA-mediated translational repression. Although reduced mRNA levels in both ectopic and endogenous miRNA regulatory interactions account for most (over 84%) of the decreased protein production (Guo et al., 2010), there is still a small part of potential miRNA/target genes that would be absent in this study. In addition, further investigations e.g., dual-luciferase reporter assay are warranted to verify the direct targeting relationship between miRNAs and mRNAs identified by high throughput screening in this study. The exact functional relevance of these miRNA-target genes in the neurotoxicity as well as neurocognitive deficits following the anesthetics exposure also needs to be deciphered in future investigations.

CONCLUSION

In conclusion, this study conducted the first miRNAs profiling coupled with their target genes identification in the dentate gyrus following isoflurane exposure. Our results indicate that a single 4 h exposure to isoflurane yields a large number of differently expressed miRNA-target genes in the dentate gyrus of P7 mice, and these miRNA/target genes may extensively mediate isoflurane-induced neurotoxicity. We believe that our results will offer novel insights into the cellular events mediated by miRNA/target genes that contribute to anesthetics-induced neurotoxicity, particularly through cell apoptosis.

ACKNOWLEDGEMENT

This work was sponsored by research grants from the National Natural Science Foundation of China (81971210 and 31671249 for Jian-Xin Liu).

REFERENCES

Altman J, Bayer SA (1990) Migration and distribution of two populations of hippocampal granule cell precursors during the perinatal and postnatal periods. J Comp Neurol 301: 365–381.

Armstrong R, Xu F, Arora A, Rasic N, Syed NI (2017) General anesthetics and cytotoxicity: possible implications for brain health. Drug Chem Toxicol 40: 241–249.

Atluri N, Ferrarese B, Osuru HP, Sica R, Keller C, Zuo Z, Lunardi N (2019) Neonatal anesthesia impairs synapsin 1 and synaptotagmin 1, two key regulators of synaptic vesicle docking and fusion. Neuroreport 30: 544–549.

Bahmad HF, Darwish B, Dargham KB, Machmouchi R, Dargham BB, Osman M, Khechen ZA, El Housheimi N, Abou-Kheir W, Chamaa F (2020) Role of microRNAs in anesthesia-induced neurotoxicity in animal models and neuronal cultures: a systematic review. Neurotox Res 37: 479–490.

Bartel DP (2004) MicroRNAs: genomics, biogenesis, mechanism, and function. Cell 116: 281–297.

Bartel DP (2018) Metazoan microRNAs. Cell 173: 20–51.

Cameron HA, Glover LR (2015) Adult neurogenesis: beyond learning and memory. Annu Rev Psychol 66: 53–81.

Fang F, Xue Z, Cang J (2012) Sevoflurane exposure in 7-day-old rats affects neurogenesis, neurodegeneration and neurocognitive function. Neurosci Bull 28: 499–508.

Fodale V, Tripodi VF, Penna O, Famà F, Squadrito F, Mondello E, David A (2017) An update on anesthetics and impact on the brain. Expert Opin Drug Saf 16: 997–1008.

Guo H, Ingolia NT, Weissman JS, Bartel DP (2010) Mammalian microRNAs predominantly act to decrease target mRNA levels. Nature 466: 835–840.

Istaphanous GK, Howard J, Nan X, Hughes EA, McCann JC, McAuliffe JJ, Danzer SC, Loepke AW (2011) Comparison of the neuroapoptotic properties of equipotent anesthetic concentrations of desflurane, isoflurane, or sevoflurane in neonatal mice. Anesthesiology 114: 578–587.

Jevtovic-Todorovic V (2005) General anesthetics and the developing brain: friends or foes? J Neurosurg Anesthesiol 17: 204–206.

Lee BH, Chan JT, Hazarika O, Vutskits L, Sall JW (2014) Early exposure to volatile anesthetics impairs long-term associative learning and recognition memory. PLoS One 9: e105340.

Levy RJ (2017) Carbon monoxide and anesthesia-induced neurotoxicity. Neurotoxicol Teratol 60: 50–58.

Li ZQ, Li LX, Mo N, Cao YY, Kuerban B, Liang YX, Fan DS, Chui DH, Guo XY (2015) Duration-dependent regulation of autophagy by isoflurane exposure in aged rats. Neurosci Bull 31: 505–513.

Loepke AW, Istaphanous GK, McAuliffe JJ 3rd, Miles L, Hughes EA, McCann JC, Harlow KE, Kurth CD, Williams MT, Vorhees CV, Danzer SC (2009) The effects of neonatal isoflurane exposure in mice on brain cell viability, adult behavior, learning, and memory. Anesth Analg 108: 90–104.

McCann ME, Soriano SG (2019) Does general anesthesia affect neurodevelopment in infants and children? BMJ 367: l6459.

Neag MA, Mitre AO, Catinean A, Mitre CI (2020) An overview on the mechanisms of neuroprotection and neuro\toxicity of isoflurane and sevoflurane in experimental studies. Brain Res Bull 165: 281–289.

Olney JW, Young C, Wozniak DF, Jevtovic-Todorovic V, Ikonomidou C (2004) Do pediatric drugs cause developing neurons to commit suicide? Trends Pharmacol Sci 25: 135–139.

Stratmann G, May LD, Sall JW, Alvi RS, Bell JS, Ormerod BK, Rau V, Hilton JF, Dai R, Lee MT, Visrodia KH, Ku B, Zusmer EJ, Guggenheim J, Firouzian A (2009) Effect of hypercarbia and isoflurane on brain cell death and neurocognitive dysfunction in 7-day-old rats. Anesthesiology 110: 849–861.

Stratmann G, Sall JW, May LD, Bell JS, Magnusson KR, Rau V, Visrodia KH, Alvi RS, Ku B, Lee MT, Dai R (2009) Isoflurane differentially affects neurogenesis and long-term neurocognitive function in 60-day-old and 7-day-old rats. Anesthesiology 110: 834–848.

Sun H, Hu H, Xu X, Tao T, Liang Z (2020) Key miRNAs associated with memory and learning disorder upon exposure to sevoflurane determined by RNA sequencing. Mol Med Rep 22: 1567–1575.

Tao G, Xue Q, Luo Y, Li G, Xia Y, Yu B (2016) Isoflurane is more deleterious to developing brain than desflurane: the role of the Akt/GSK3β signaling pathway. Biomed Res Int 2016: 7919640.

Xia Y, Xu H, Jia C, Hu X, Kang Y, Yang X, Xue Q, Tao G, Yu B (2017) Tanshinone IIA attenuates sevoflurane neurotoxicity in neonatal mice. Anesth Analg 124: 1244–1252.

Xiao XL, Wu JT, Zhang HZ, Wang YD, Zhang JQ, Liu LF, Yu-Chen, Min-Li, Yang PB, Wu XL, Liu JX (2021) The neurotoxic effect of isoflurane on age-defined neurons generated from tertiary dentate matrix in mice. Brain Behav 11: e01949.

Xu J, Xu M, Wang Y, Mathena RP, Wen J, Zhang P, Furmanski O, Mintz CD (2019) Anesthetics disrupt growth cone guidance cue sensing through actions on the GABAA α2 receptor mediated by the immature chloride gradient. Neurotoxicol Teratol 74: 106812.